

A Low Cost Electrically Tunable Bandpass Filter with Constant Absolute Bandwidth

Dwipjoy Sarkar *, Tamasi Moyra

National Institute of Technology Agartala , Jirania 799046, India

* Corresponding author (E-mail: dwipjoysarkar@gmail.com)

Abstract

This paper presents an electrically tunable bandpass filter which provides nearly constant absolute bandwidth (CABW) within the center frequency tuning range. The proposed tunable band pass filter (BPF) is designed on a low cost FR4 substrate with mixed coupled 3rd order open loop ring resonators, high frequency varactor diodes, chip capacitors and some RF chokes. The center frequency of the BPF is tunable from 1.9 GHz to 2.52 GHz with 3 dB absolute bandwidth of 201.5 ± 1.5 MHz. The measured insertion loss of the proposed BPF is found less than 3 dB within the tuning range. There is a good agreement found between the simulated and measured results of the proposed BPF.

Keywords

Microstrip; BPF; CABW; resonator; scattering; tunable

1. Introduction

Tunable microwave and RF bandpass filters (BPFs) are subject of interest to improve adaptability in communication systems. Microstrip BPFs can be tuned electrically, magnetically or by using MEMS based switches. Electrical or MEMS based tuning methods are mostly preferred because of higher fabrication density obtained with these methods. This present work is based on electrical tuning of microstrip BPF using varactor diodes. Some recently published articles based on tunable microstrip BPFs are shown in [1-17]. Tunable BPFs can be divided into single passband and dual passband type with center frequency tunability, bandwidth tunability, constant absolute bandwidth (CABW) and constant fractional bandwidth (CFBW) types respectively. Center frequency tunable microstrip BPFs with single passbands are proposed in [1-3] using [1] microstrip line ring resonator with varactor diodes, [2] open loop ring resonator with piezoelectric transducer (PET), and [3] microstrip lumped elements with varactor loaded inductors respectively. Center frequency tunable BPFs with switchable bandwidth and continuously tunable bandwidth are proposed in [4-5] using [4] varactor and pin diode loaded with dual mode resonators and [5] combline topology with variable coupling reducers. Although the center frequencies of the BPFs shown in [1-5] are tunable but the passband characteristics are not similar for the tuning range. Therefore, the concepts of center frequency tunable BPFs with CABW and CFBW are

evolved to preserve the passband characteristics within the tuning range. Article [6] presents, a two and three-pole microstrip 'LC' CFBW and CABW tunable BPF. The equivalent-circuit models are presented to study the tunable mechanism. The electric coupling coefficient is compensated to control the overall coupling, but the control of external quality factor is not shown which is also necessary to obtain constant bandwidth. Some other types of CABW BPF with single passbands are proposed in [7-11] using [7] varactor loaded open circuit resonators, [8] varactor tuned corrugated coupled line resonators, [9] varactor tuned quarter wavelength resonators with mixed coupling architecture, [10] varactor-loaded parallel coupled microstrip resonators and [11] simulated lumped elements loaded with varactor diodes respectively. Tunable microstrip BPFs can be also achieved for dual band applications as shown in [12-17], which are based on [12] quarter wavelength resonators, [13] stepped impedance resonators with loaded stubs, [14] centrally coupled resonator (CCR), [15] quadruple mode stub loaded resonator, [16] stub loaded half wavelength resonators and [17] dual mode resonators respectively.

Although undoubtedly, enormous researches have been already conducted on tunable CABW BPF or both the center frequency and bandwidth tunable BPF, further research is still required for the development of cost effective tunable BPF having wider bandwidth and uniform passband characteristics. In this present work, a low cost and electrically tunable microstrip BPF with CABW is proposed. The proposed BPF consists of three half wavelength mix coupled open loop microstrip ring resonators, SMV 2019-079LF varactors, ultra high frequency chip capacitors and RF chokes. The odd mode resonant frequency of the filter is tunable from 1.9 to 2.52 GHz with 3 dB absolute bandwidth of 201.5 ± 1.5 MHz. The electric coupling coefficient and external quality factor of the BPF is controlled to achieve nearly constant absolute bandwidth. The optimized BPF provides less than 3 dB insertion loss, 32.6 % tunability, (201.5 ± 1.5) MHz absolute bandwidth (ABW) with only 1.48 % ABW variation within the tuning range of (1.9 GHz – 2.52 GHz). EM and circuit simulations are carried out in Sonnet software. The proposed BPF is fabricated on an FR4 substrate ($\epsilon_r = 4.4, h = 1.6\text{mm}, \tan \theta = 0.02$) and the measured results obtained by the Agilent N5221A Vector Network Analyzer (VNA) shows good agreement with the simulated results.

2. Design and analysis of the proposed tunable BPF

Fig. 1 depicts the theoretical layout of the proposed 3rd order tunable BPF. The physical dimensions of the BPF are shown in Table 1. The BPF is constructed using FR4 substrate ($\epsilon_r = 4.4, h = 1.6\text{mm}, \tan \theta = 0.02$), varactor diodes (C_v), fixed capacitors (C, C_1) and RF chokes. The variable capacitors (C_v) are SMV 2019-079LF varactor diodes from Skyworks Solutions. The capacitance is variable from 0.3 pF – 2.22 pF under (20V – 0V) reverse bias voltage variations. All the fixed capacitances are realized using 0.4 pF Murata high frequency chip capacitors. The bias voltages and ground lines are connected to the filter circuit by means of RF chokes to restrict the RF signal from entering into the biasing circuitry. The detailed analysis and design procedure of the proposed BPF are discussed in sub sections 2.1, 2.2 and 2.3 respectively.

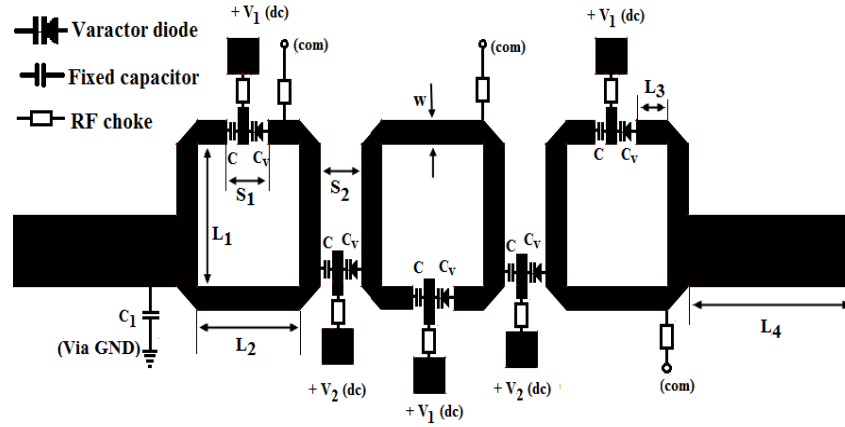


Fig. 1. Layout of the proposed 3rd order tunable BPF

Table 1- Dimensions of the 3rd Order BPF

Dimensions	
Lengths (L_1, L_2, L_3, L_4)	(5.9, 5, 1.5, 10) mm
Width (w)	(1) mm
Spacing (S_1, S_2)	(2,2) mm

2.1. Resonance property of the open loop ring resonator

Fig. 2 (a) depicts an open loop ring resonator with 45° chamfered bends. An ideal capacitor C is used to represent the gap between the resonator arms. The decoupled odd and even mode equivalent circuit of the resonator is shown in Fig. 2(b) and Fig. 2(c) respectively. From the equivalent circuits, it is found that the odd mode resonant frequency can be changed by varying the gap capacitance C .

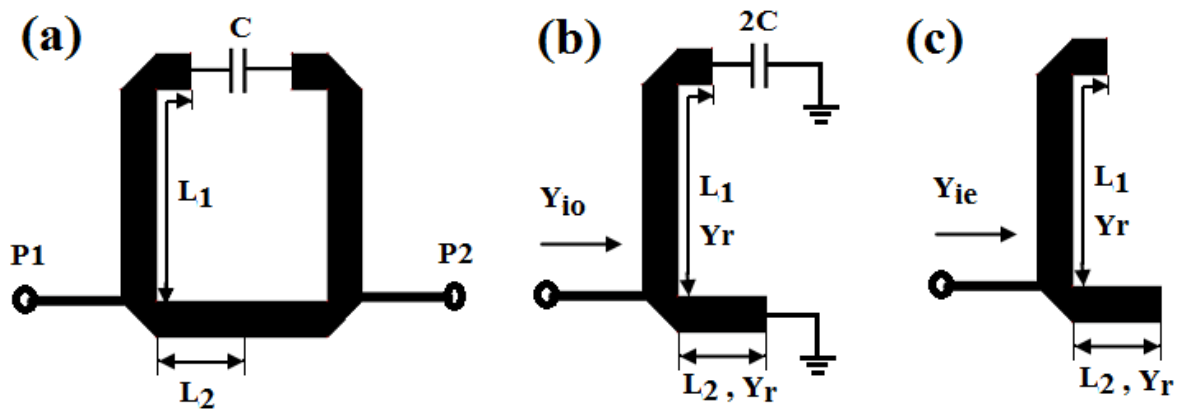


Fig. 2- (a) Open loop resonator; (b) Odd mode equivalent circuit; (c) Even mode equivalent circuit

By ignoring all the parasitic effects and radiation from the transmission line segments, the odd mode input admittance Y_{io} for Fig. 2 (a) can be found as:

$$Y_{io} = \frac{2j\omega CY_r + jY_r^2 \tan \beta L_1}{Y_r - 2\omega C \tan \beta L_1} - jY_r \cot \beta L_2 \quad (1)$$

Where, ω is angular frequency, β is propagation constant, and Y_r is the characteristic admittance of the microstrip lines L_1 and L_2 .

The odd mode resonant frequency can be solved from equation (1) by putting $Y_{io} = 0$, which gives:

$$2j\omega CY_r (1 + \cot \beta L_2 \tan \beta L_1) + jY_r^2 (\tan \beta L_1 - \cot \beta L_2) = 0 \quad (2)$$

Now the relationship between capacitance (C) and odd mode frequency (f_o) can be found

by placing $\beta = \frac{2\pi f_o \sqrt{\epsilon_e}}{v_l}$ and $\omega = 2\pi f_o$ in equation (2), which gives:

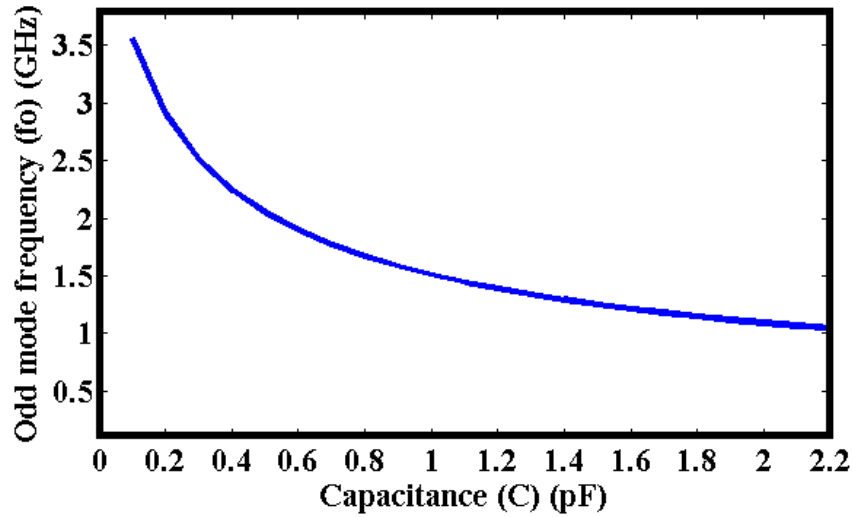
$$C = \frac{Y_r}{4\pi f_o \tan \left[\frac{2\pi f_o}{v_l \sqrt{\epsilon_e}} (L_1 + L_2) \right]} \quad (3)$$

Where, f_o = odd mode resonant frequency, ϵ_e = effective dielectric constant = $\frac{\epsilon_r + 1}{2} + \frac{\epsilon_r - 1}{2} (1 + 12h/w)^{1/2}$, v_l = velocity of light, ϵ_r = Relative permittivity, w = strip width, h = substrate height.

For a particular case of ring resonator parameters shown in Table 2, the capacitance (C) and odd mode resonant frequency (f_o) characteristic is obtained using equation (3), which is depicted in Fig. 3. It can be found that the odd mode resonant frequency (f_o) is monotonically decreased with the increment of capacitance C and therefore a commercial FR4 substrate ($\epsilon_r = 4.4, h = 1.6\text{mm}, \tan \theta = 0.02$) can be easily used to obtain tunability in the lower frequency range (1 GHz – 3.5 GHz) by varying the capacitance in between (2.2 pF – 0.2pF).

Table 2 - Ring Resonator Parameters

Resonator Parameters	
Lengths (L_1, L_2)	(7, 2.5) mm
Admittance (Y_r)	(1/87.23) mho
Substrate (ϵ_r, h)	(4.4, 1.6 mm)

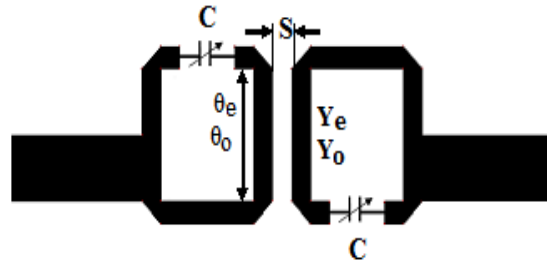
Fig.3. Capacitance (C) vs. odd mode resonant frequency (f_o) plot

2.2. Achievement of CABW property

Fig. 4 illustrates the 2nd order tunable filter using mixed coupled ring resonators. The mutual coupling coefficient (k) for this arrangement can be found [18] as:

$$k = |k_e - k_m| \quad (4)$$

Where, k_e is electric coupling coefficient and k_m is magnetic coupling coefficient.

Fig.4. 2nd Order tunable BPF

On the other hand, the mutual coupling coefficient (k) and the external quality factor (Q_e) for a conventional coupled resonator BPF can be found [18] as:

$$k = \frac{BW}{f_0 \sqrt{g_i g_{i+1}}}, i = 1 \dots (n-1) \quad (5)$$

$$Q_e = \frac{g_0 g_1 f_0}{BW} \quad (6)$$

Where, BW is 3 dB absolute bandwidth, f_0 is the center frequency and g_0, g_1, g_i and g_{i+1} are filter coefficients.

From equations (5) and (6) it can be found that the bandwidth (BW) is proportionally related with the center frequency (f_0) of the BPF and it can be made constant if the mutual coupling coefficient (k) is inversely varied whereas the external quality factor (Q_e) is proportionally varied with the center frequency. Fig. 5 and Fig. 6 illustrate such arrangements for the fulfilment of the above mentioned objective.

From equation (4) it can be observed that either the electric or magnetic coupling coefficient has to be varied to control the overall coupling coefficient. It is more convenient to vary the electric coupling coefficient rather than the magnetic coupling coefficient. A tunable capacitor can be utilised to control the electric couplings between the gaps of adjacent resonators. Fig. 5 (a) represents the equivalent circuit [18] of a coupling gap.

In Fig. 5 (b), the coupling gap is loaded with a tunable capacitor and therefore the equivalent circuit is accordingly modified.

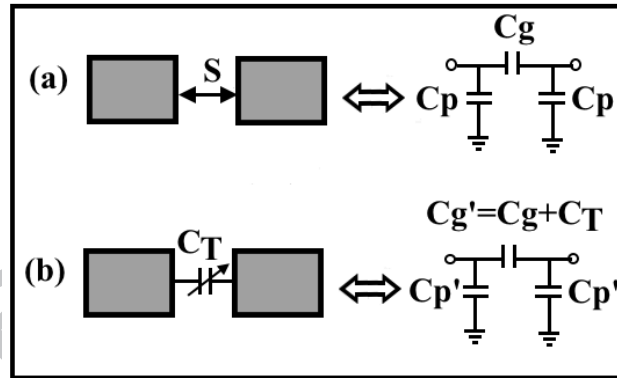


Fig. 5 - (a) Equivalent circuit of coupling gaps and (b) Modified coupling with tunable capacitor

From [18], the approximate formulas for series and parallel branch capacitances can be written as:

$$C_p' = 0.5C_e \quad (7)$$

$$C_g' = 0.5C_o - 0.25C_e \quad (8)$$

Where C_e and C_o are even and odd mode capacitances.

The electric coupling coefficient can be calculated by the formula provided for mixed coupling in [18] as:

$$k_e = \frac{C_m}{\sqrt{C_1 C_2}} \quad (9)$$

From the Fig. 5 (b) and [18], C_m , C_1 and C_2 can be found as:

$$C_m = C_g' \quad (10)$$

$$C_1 = C_2 = C_p' + C_m \quad (11)$$

Now the electric coupling coefficient (k_e) can be solved using equations (7), (8), (9), (10) and (11) as:

$$k_e = \frac{C_g'}{C_g' + C_p'} = \frac{C_g + C_T}{C_g + C_T + C_p'} \quad (12)$$

From equation (12), it is clear that the capacitance (C_T) must be set to a lower value to reduce the electric coupling coefficient (k_e). The reduced electric coupling coefficient (k_e) results in the reduction of overall coupling coefficient (k). The reduced overall coupling coefficient (k) can fix the bandwidth change due to center frequency tuning and therefore the absolute bandwidth can be made constant accordingly.

Fig. 6 depicts the external quality factor (Q_e) adjustment technique. The external quality factor (Q_e) should increase while the resonant frequency (f_0) is tuned upward. The external quality factor of a resonator can be calculated theoretically [18] as:

$$Q_e = \frac{\omega_0}{2Y_r} \left| \frac{\partial \text{Im}[Y_{in}(\omega)]}{\partial \omega} \right|_{\omega=\omega_0} \quad (13)$$

The odd mode equivalent circuit of Fig. 2 (a) is loaded with another capacitor (C_T') near the feed line.

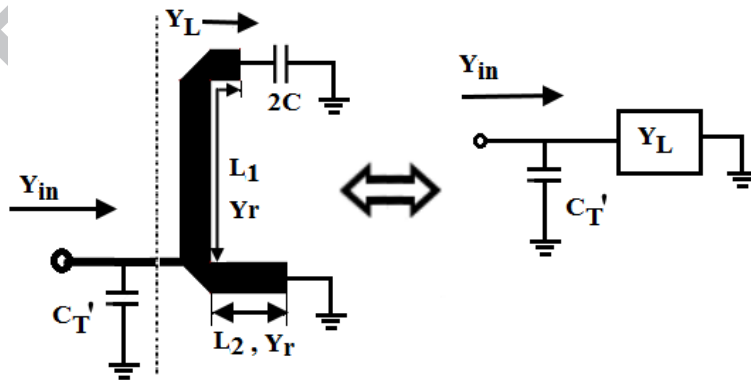


Fig.6. External quality factor adjustment technique

The external quality factor (Q_e) for Fig. 6 can be found using equation (13) as:

$$Q_e = \frac{\omega_0}{2Y_r} \left| C_T' + \frac{\partial}{\partial \omega} \{ \text{Im}(Y_L) \} \right|_{\omega=\omega_0} \quad (14)$$

In the above equation ' $\text{Im}(Y_L)$ ' is the imaginary part of ' Y_{io} ' (equation 1). The additional capacitance (C_T') of equation (14) can be used to control the external quality factor (Q_e).

The tunability characteristics of the electric coupling coefficient (k_e) and the external quality factor (Q_e) are extracted using equations (12) and (14), which are depicted in Fig. 7(a) and Fig. 7(b) respectively. The electric coupling coefficient (k_e) is non-linearly varied with C_T whereas the external quality factor (Q_e) is almost linearly varied with C_T' .

On the other hand, the overall required coupling coefficient (k) and external quality factor (Q_e) for the 2nd order CABW BPF ($g_0 = 1$, $g_1 = 1.1468$, $g_2 = 1.1732$, and $BW = 200$ MHz) against different resonance frequencies are extracted using weakly coupled structure, which are depicted in Fig. 7(c) and Fig. 7(d) respectively. It can be found that the desired and obtained (k, Q_e) values are very close and therefore the criteria for maintaining the CABW are satisfied.

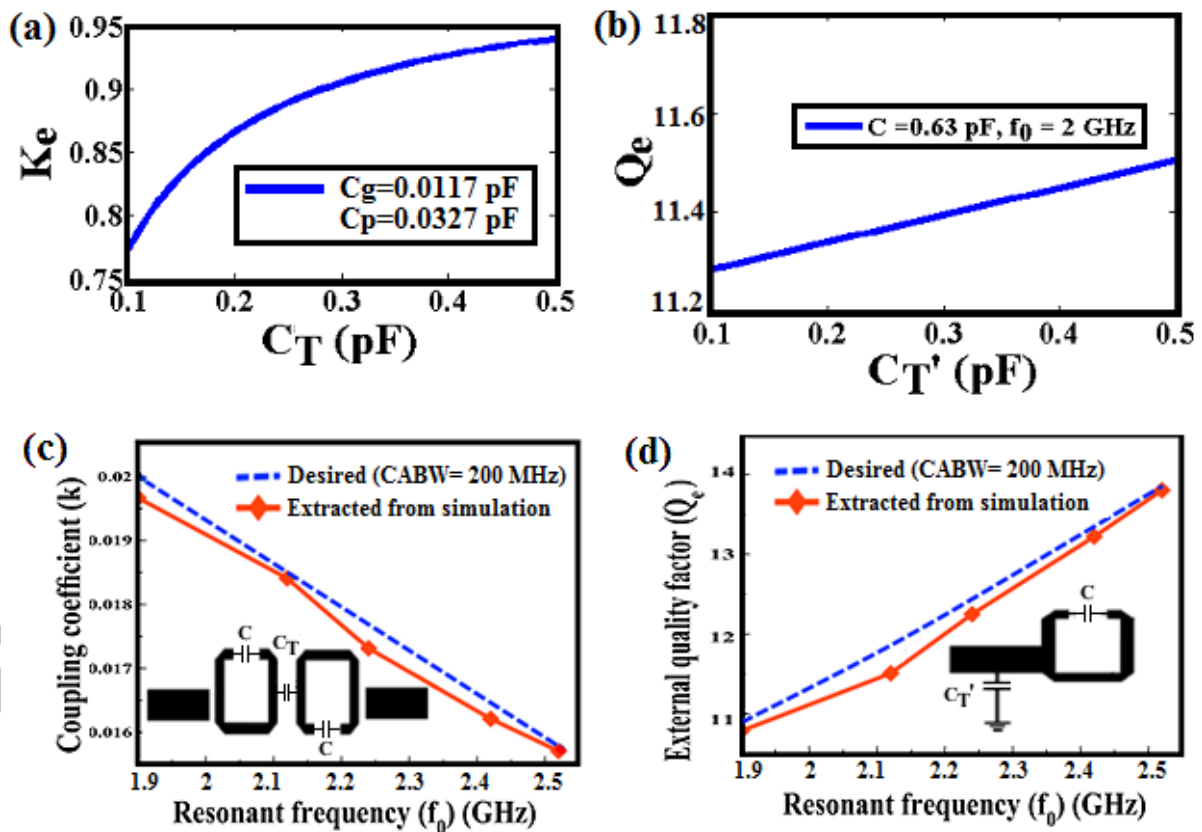


Fig.7 - (a) Electric Coupling coefficient (k_e) against C_T ; (b) External quality factor (Q_e) against C_T' ; (c) Coupling coefficient (k) against resonant frequency (f_0); (d) External quality factor (Q_e) against resonant frequency (f_0)

3. Simulation and experimental validation

Fig. 8 (a) depicts the fabricated layout of the proposed high selective 3rd order tunable BPF. The combination of capacitors C and C_v in Fig.8 is equivalent to the capacitor C of Fig. 2. The spice model of the SMV 2019-079LF varactor diode(C_v) is illustrated in Fig.8 (b). In Fig. 8 (a), the capacitor C is utilized to block the DC from entering into the RF circuitry. The optimized value of the fixed capacitance C_1 is 0.4 pF for which the external quality factor has been increased within the tuning range and it is determined by the full wave electromagnetic (EM) simulations. The capacitance C_1 is only connected to the input feed line for reducing the additional losses due to soldering and nonlinearity, however it can be connected to both the input and output feed terminals with the capacitance value distributed as $C_1/2$. The full wave EM Simulations are carried out in Sonnet software and all the measurement results of the fabricated BPF are obtained using Agilent N5221A VNA.

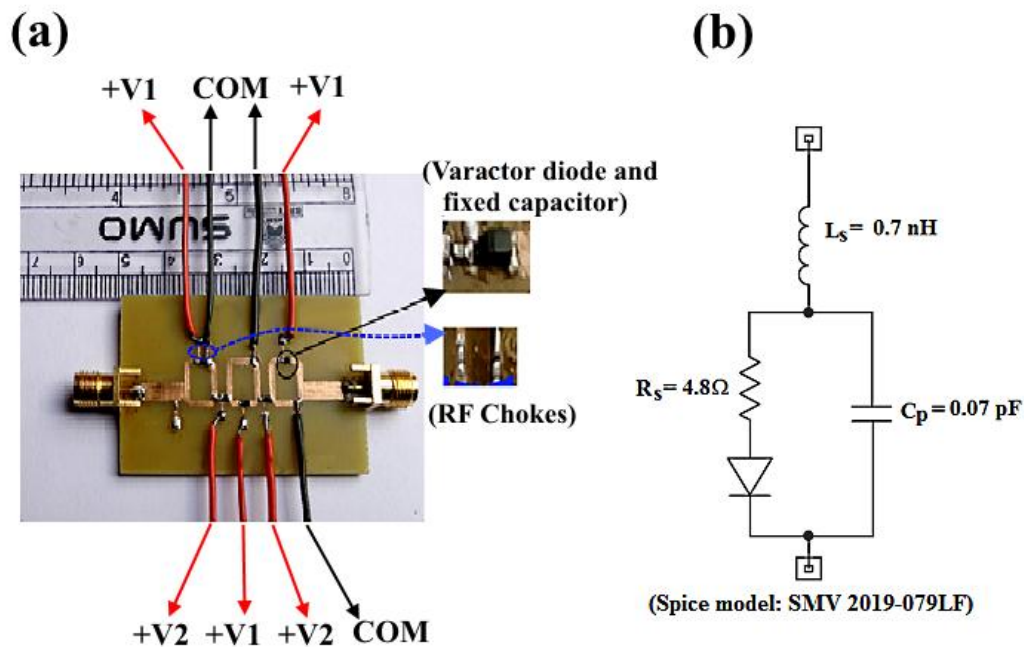


Fig.8 - (a) Photograph of the fabricated filter; (b) Spice model of SMV 2019-079LF varactor diode.

Fig. 9 (a) and Fig. 9 (b) depict the scattering response (S_{21}, S_{11}) of the proposed tunable BPF. The resonant frequency of the BPF is varied from 1.9 GHz to 2.52 GHz for different applied bias voltages (V_1) ranging from 0 volt to 20 volt. The resonant frequency versus bias voltage (V_1) characteristic is illustrated in Fig. 9(c). The resonant frequency is varied non-linearly with the applied voltage V_1 . Due to the increment of V_1 , the capacitance of the varactor diode is reduced and it accordingly increases the resonant frequency of the BPF.

The bias voltages labelled $+V_1$ in Fig. 8 are varied at the same time to tune the resonant frequency whereas the $+V_2$ lines are used to tune the bandwidth of the BPF. The five different tuned center frequencies of the proposed BPF are found at 1.9 GHz, 2.12 GHz, 2.24 GHz, 2.42 GHz and 2.52 GHz with 3 dB absolute bandwidths as 200 MHz, 200 MHz, 200MHz, 201 MHz and 203 MHz for the applied bias voltages (V_1, V_2) as (0, 0), (2, 2), (4, 4), (9, 5) and (20, 5) volts respectively. The 3 dB average absolute bandwidth of the BPF is

found 201.5 ± 1.5 MHz within the entire tuning range. The measured insertion loss of the BPF is varied from 1.5 dB to 2.7 dB in the full tuning bandwidth whereas the return loss is better than 12 dB.

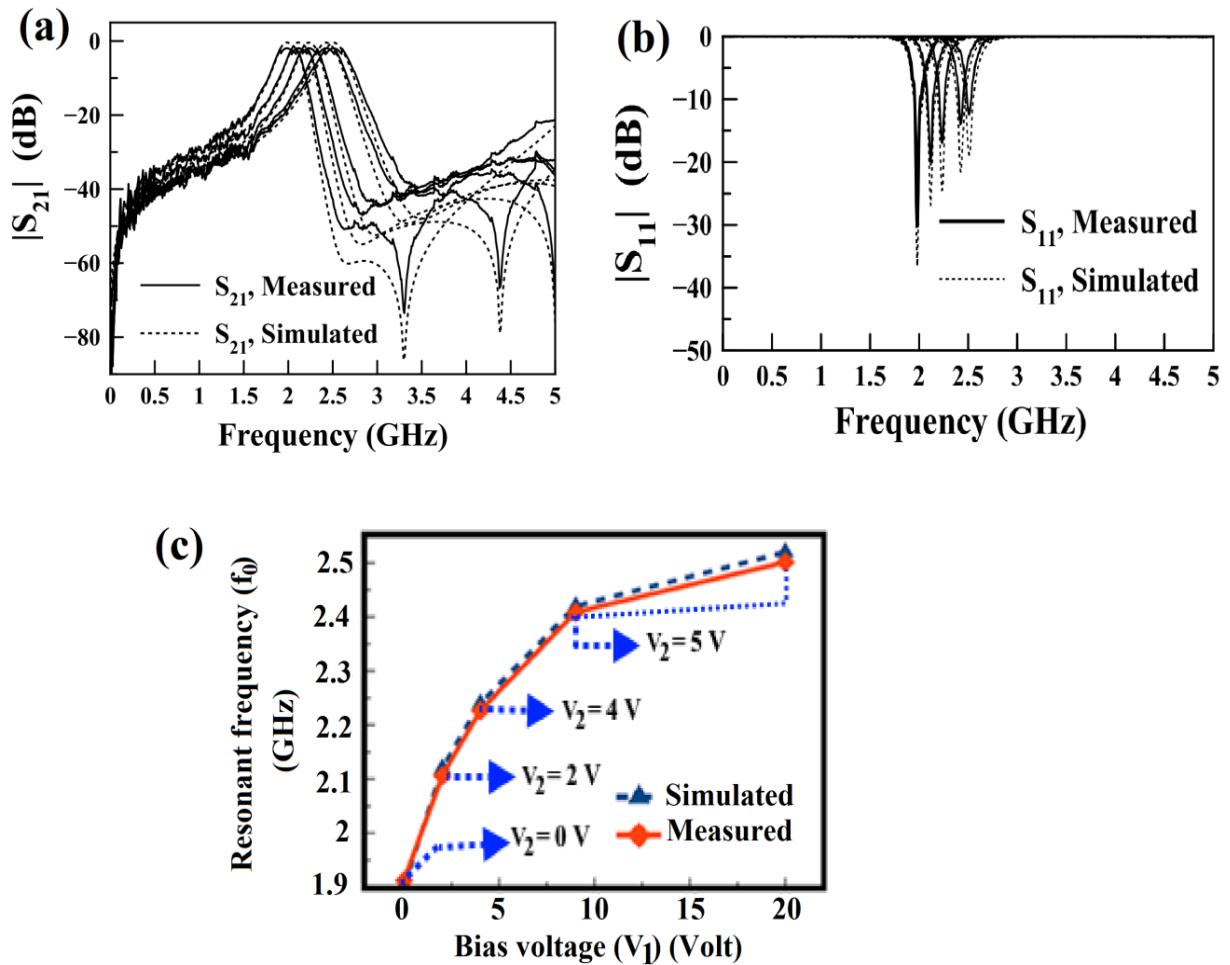


Fig. 9 - (a) Scattering response, $|S_{21}|$; (b) Scattering response, $|S_{11}|$; (c) Resonant frequency (f_0) versus bias voltage ($+V_1$) characteristics

The center frequency and bandwidth tuning steps of the proposed tunable BPF are illustrated in Fig. 10 (a) and Fig. 10 (b) respectively using flowchart diagrams. The center frequency of the BPF can be tuned in the upward and downward direction by increasing and decreasing the bias voltages in the $+V_1$ lines. On the other hand, the 3 dB bandwidth of the BPF can be made wider or narrower by decreasing and increasing the bias voltages in the $+V_2$ lines. All the voltages (V_1 , V_2) should be kept fixed when the desired center frequency and bandwidth is achieved.

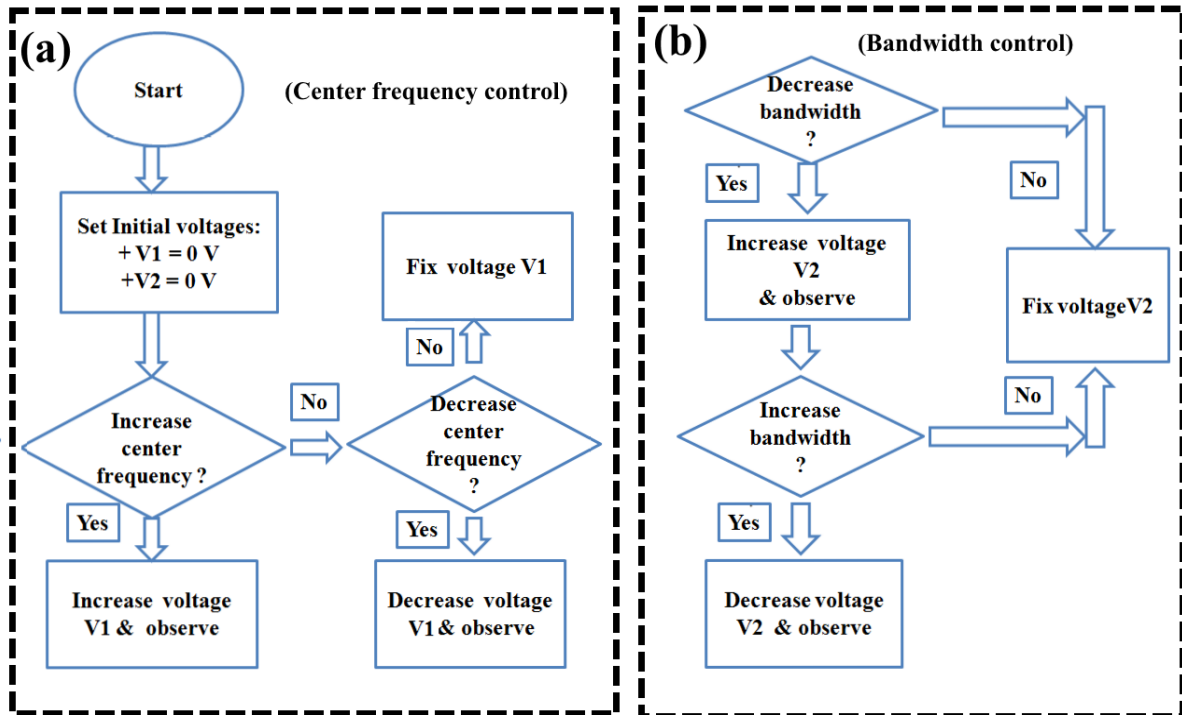


Fig.10 - (a) Center frequency control flowchart; (b) bandwidth control flowchart

Fig. 11 (a) depicts the plot of ABW for different center frequencies. It can be found that from 1.9 GHz to 2.2 GHz, the plot is like a straight line with a slope almost near to zero and has the significance of zero bandwidth variation within this range. Between 2.2 GHz to 2.52 GHz, some slope changes can be found which represents slight bandwidth variation within this range.

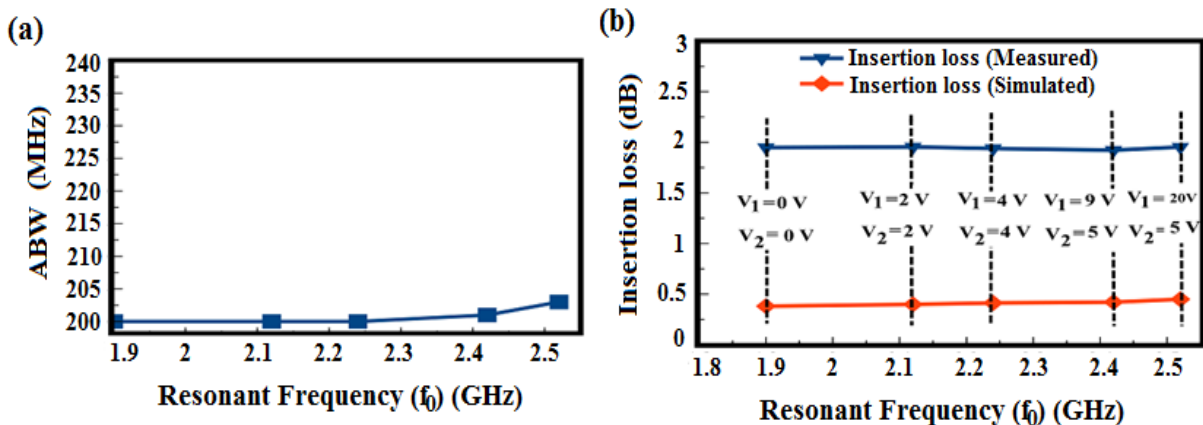


Fig.11 - (a) Absolute bandwidth at different resonant frequencies; (b) Insertion loss at different resonant frequencies

Fig. 11 (b) illustrates the insertion loss characteristic of the proposed CABW BPF. The insertion loss of the simulated BPF is found from 0.4 dB to 0.5 dB at different resonant frequencies whereas it is always less than 1 dB in the passband. On the other hand, the insertion loss of the measured BPF is around 1.9 dB to 2 dB at different resonant frequencies meanwhile it is always less than 3 dB in the passband. The increased insertion loss of the fabricated BPF is due to additional losses of SMA connectors, non linearity of lumped components, fabrication tolerances and radiation losses.

The overall performance comparison of the proposed CABW BPF along with others' design is shown in Table 3. It can be found that the proposed tunable BPF in this work provides wider bandwidth and lesser passband insertion loss compared to [5], [7], [8] and [9] with measured bandwidth variation comparatively smaller than [5], [8] and [9] respectively.

Table 3 - Performance comparison

Ref.	Substrate Used ($\epsilon_r, h, \tan\theta$)	f_0 (GHz)	3dB Bandwidth (MHz)	Insertion loss (dB)
	Teflon:			
[5]	(2.2, 0.256, 0.00028)	0.47–0.862	5–15	> 3
	RT/D 6010:			
[7]	(10.2, 1.27, 0.0023)	0.78–1.08	49±1	2.9 – 3.4
	RT/D 6006:			
[8]	(6.15, 0.62, 0.0019)	1.45–1.89	70±4	2.50 – 2.92
	Duroid R4350B:			
[9]	(3.6, 0.254, 0.0031)	0.9–1.5	74±15	4.5 – 5.9
This work	FR4: (4.4, 1.6, 0.02)	1.9 – 2.52	201.5±1.5	1.5–2.7

5. Conclusions

In this article an electrically tunable microstrip BPF with nearly constant 3 dB absolute bandwidth of 201.5±1.5 MHz is proposed. The center frequency of the BPF is tunable from 1.9 GHz to 2.52 GHz with 1.5 to 2.7 dB passband insertion loss and 1.48% bandwidth variations within the tuning range. The BPF is fabricated using FR4 substrate, SMV 2019-079 LF varactors and high frequency chip capacitors. The measured results of the proposed BPF well agree with the simulated results and can be used in Wireless LAN and other low cost communication devices.

Acknowledgment

The authors are very grateful to the editors and reviewers for their precious and productive comments which have been utilized to improve the quality of this manuscript. The authors also would like to acknowledge Mr. P. Mondal of IEST, Shibpur and Mr. L. Murmu of ISM, Dhanbad for supporting this work.

References

- [1] Makimoto, M., Sagawa, M., n.d. Varactor Tuned Bandpass Filters Using Microstrip-Line Ring Resonators. MTT-S International Microwave Symposium Digest.
- [2] Hsieh, L.-H., Chang, K., 2003. Tunable microstrip bandpass filters with two transmission zeros. *IEEE Transactions on Microwave Theory and Techniques* 51, 520–525.
- [3] Hejazi, Z.M., Jiang, Z., Excell, P.S., 2003. Lumped-element microstrip narrow bandpass tunable filter using varactor-loaded inductors. *International Journal of Electronics* 90, 57–63.
- [4] Liu, B., Wei, F., Zhang, H., Shi, X., Lin, H., 2011. A Tunable Bandpass Filter with Switchable Bandwidth. *Journal of Electromagnetic Waves and Applications* 25, 223–232.
- [5] Sanchez-Renedo, M., Gomez-Garcia, R., Alonso, J., Briso-Rodriguez, C., 2005. Tunable combline filter with continuous control of center frequency and bandwidth. *IEEE Transactions on Microwave Theory and Techniques* 53, 191–199.
- [6] Xiang, Q., Feng, Q., Huang, X., Jia, D., 2013. Electrical Tunable Microstrip LC Bandpass filters with constant bandwidth, *IEEE Transactions on Microwave Theory and Techniques* 61, 1124–1130.
- [7] Liu, B., Wei, F., Wu, Q. Y., Shi, X. W., 2011. A Tunable Bandpass filter with constant absolute bandwidth, *Journal of Electromagnetic Waves and Applications* 25, 1596–1604.
- [8] El-Tanani, M. A., Rebeiz, G. M., 2010. Corrugated Microstrip Coupled Lines for Constant Absolute Bandwidth Tunable Filters, *IEEE Transactions on Microwave Theory and Techniques* 58, 956-963.
- [9] Stefanini, R., Chatras, M., Blondy, P., 2012. Compact 2-pole and 4-Pole 1.5–0.9 GHz constant absolute bandwidth tunable filters, *IEEE MTT-S International Microwave Symposium Digest (MTT)*, 1-3.
- [10] Huang, X., Feng, Q., Zhu, L., Xiang, Q., Jia, D., 2014. Synthesis and design of tunable bandpass filters with constant absolute bandwidth using varactor-loaded microstrip resonator, *International Journal of RF and Microwave Computer-Aided Engineering* 24, 681–689.
- [11] Gohari, S.A., Dousti, M., Mafinezhad, K., 2016. A Novel Analytical Technique to design a Constant Absolute Bandwidth Bandpass Filter, *AEU- International Journal of Electronics and Communications* 70, 1433–1442.

- [12] Djoumessi, E. E., Chaker, M., Wu, K., 2009. Varactor-tuned quarter-wavelength dual-bandpass filter, *IET Microwaves, Antennas & Propagation* 3, 117–124.
- [13] Zhang, L., Wang, X.-H., Wang, Z.-D., Bai, Y.-F., Shi, X.-W., 2013. Compact electronically tunable microstrip dual-band filter using stub-loaded SIRs, *Journal of Electromagnetic Waves and Applications* 28, 39–48.
- [14] Cui, H., Sun, Y., Wang, W., Lu, Y.-L., 2015. Dual-band tunable bandpass filter with independently controllable centre frequencies, *International Journal of Electronics Letters* 4, 336–344.
- [15] Liu, H., Wen, P., Zhu, S., Ren, B., 2016. Independently controllable dual-band microstrip bandpass filter using quadruple-mode stub-loaded resonator, *International Journal of RF and Microwave Computer-Aided Engineering* 26, 602–608.
- [16] Pal, B., Dwari, S., 2017. Microstrip dual-band bandpass filter with independently tunable passbands using varactor-tuned stub loaded resonators. *AEU - International Journal of Electronics and Communications* 73, 105–109.
- [17] Jia, D., Feng, Q., Huang, X., Xiang, Q., 2014. A constant absolute bandwidth filter with dual independent tunable passbands, *IEEE International Wireless Symposium (IWS) 2014*, 1- 4.
- [18] Hong, J.-S., Lancaster, M. J., 2011. *Microstrip filters for RF/microwave applications*, 2nd ed. United States: Wiley, John & Sons.

Vitae

(Corresponding author)



Dwipjoy Sarkar was born in Agartala, India, in 1990. He received B.E. degree in Electronics and Communication Engineering from the Tripura Institute of Technology in 2012 and M.Tech degree in Communication Engineering from National Institute of Technology, Agartala in 2014. He is currently pursuing Ph.D from National Institute of Technology, Agartala. His current research interest is microstrip circuits, antennas, defected ground structures, defected microstrip structures, meta-materials, and computational electromagnetics.



Tamasi Moyra (1978) received the AMIE (India) degree in Electronics and Communication Engineering from Institution of Engineers, India in the year 2003. She did M.E. in the year 2007 from Bengal Engineering and Science University, Shibpur, India in the Department of Electronics and Telecommunication Engineering. She received the Ph.D degree in the year of 2014 from department of Electronics and Telecommunication Engineering at Indian Institute of Engineering Science and Technology (IEST), Shibpur, India. Presently, she is working as an Assistant Professor in the Department of Electronics and Communication Engineering at National Institute of Technology, Agartala. She has published more than 19 research articles in different peer reviewed journals, international conferences and book chapters. Her current research interests include the planar circuits, Microstrip filters, antenna elements, LHM, meta-materials etc. She is a life member of Institution of Engineers, India.